increased trimethylated histone H3 at Lys27 (H3-K27Me3), which correlates with genomic silencing was detected in Menin$^{-/-}$ Th17 cells (Fig. 3*C*, *Left*). In sharp contrast, loss of Menin had little effect on epigenetic histone modifications at the *Rorc* locus (Fig. 3*C*, *Center*).

Menin interacts specifically with RNAPII (34). In addition, eukaryotic gene expression is regulated by RNAPII through the phosphorylation of its carboxyl-terminal domain (CTD) (35). Ser-2 phosphorylation (2P) marks the elongation state, whereas Ser-5 is phosphorylated (5P) in the initiation phase (36). Therefore, we examined whether Menin is required for the recruitment of RNAPII to the *Il17a* gene locus in Th17 cells. The binding levels of Menin to the *Il17a* and *Rorc* gene loci in WT Th17 cells restimulated with an immobilized anti-TCRβ were similar to the binding levels in cells that had not been restimulated (Fig. 3*D*, *Upper*). Interestingly, however, the recruitment of RNAPII to the *Il17a* gene locus, but not to the *Rorc* gene locus, was markedly up-regulated after TCR restimulation (Fig. 3*D*, *Lower*, and Fig. S4*D*, *Bottom*). This is consistent with the observation that *Il17a* expression, but not *Rorc*, was up-regulated by TCR restimulation (Fig. 3*E*). The H3-K4Me3 and H3-K9Ac histone modifications at these gene loci were not altered by TCR restimulation (Fig. S4*D*, *Top* and *Middle*). Next, we assessed whether Menin was required for recruitment of RNAPII to the *Il17a* and *Rorc* gene loci. Compared with WT cells, the levels of RNAPII Ser-5 and Ser-2 phosphorylation together with a total RNAPll at the *Il17a* gene were much lower in Menin$^{-/-}$ Th17 cells restimulated with anti-TCRβ antibody (Fig. 3*F*). In contrast, the reduction of RNAPII at the *Rorc* gene locus in Menin$^{-/-}$ Th17 cells was much less dramatic. These results indicate that, in Th17 cells, Menin is primarily required for RNAPII accumulation and Ser-2/Ser-5 double phosphorylation at the *Il17a* gene locus.

STAT3 directly regulates not only gene expression but also epigenetic modifications of numerous genes involved in Th17 cell differentiation (37, 38). In the case of the *Il17a* and *Rorc* gene loci, STAT3 directly binds the promoter and also intergenic regions and induces alterations to the epigenetic signature of these genes. Consistent with these studies (37, 38), loss of STAT3 resulted in the disappearance of IL-17A–producing cells (Fig. S5*A*). The binding of STAT3 to *Il17a* and *Rorc* gene loci in Menin$^{-/-}$ Th17 cells was similar to that in WT cells (Fig. S5*B*). However, the binding of Menin to these loci in STAT3$^{-/-}$ Th17 cells was reduced (Fig. S5*C*). IL-6 stimulation alone could not induce Menin accumulation at the *Il17a* locus (Fig. S5*D*). These results indicate that STAT3 binding to the *Il17a* and *Rorc* gene loci was independent of Menin expression, whereas STAT3 in combination with TGF-β stimulation is required for the recruitment of Menin to these two gene loci.

Menin Is Crucial for Maintaining the Expression of *Rorc* and Permissive Histone Modifications at the *Rorc* Gene Locus in Differentiated Th17 Cells. We have previously shown that, once Th2 cell differentiation takes place, *Gata3* expression and Th2 function is maintained via recruitment of the Menin/TrxG complex to the *Gata3* gene locus, even in the absence of IL-4–mediated STAT6 activation (23). We examined whether the expression of *Rorc* is maintained in a similar fashion via the binding of the Menin/TrxG complex in an IL-6/STAT3-independent manner. As TGF-β1 has been shown to be important, and IL-6 has been shown to be dispensable for the maintenance of IL-17A expression by Th17 cells (39), we cultured Th17 cells in the absence of IL-6 after the first cycle of Th17 differentiation. After initial differentiation, Th17 cells generated from WT T cells maintained the ability to produce IL-17A throughout two extra cycles of culture in the absence of IL-6 (Fig. 4*A*, *Upper*). Decreased numbers of IL-17A–producing cells and decreased expression of the *Il17a* gene were also observed throughout the culture period in Menin$^{-/-}$ Th17 cells compared with WT Th17 cells (Fig. 4 *A*, *Lower*, and *B*). The addition of IL-6 or IL-23 to the second culture did not rescue the number of IL-17A–producing Menin$^{-/-}$ cells (Fig. S6*A*; see 66.0% vs. 32.6% or 67.0% vs. 36.1%). The levels of histone H3-K4Me3 and H3-K9Ac at the *Il17a* gene locus were also lower in Menin$^{-/-}$ Th17 cells after the second cycle of culture without IL-6, and this defect appeared to be even more pronounced compared with that observed after initial differentiation (Figs. 3*C*, *Left*, and 4*C*, *Left*). The levels of H3-K27Me3 were also higher in Menin$^{-/-}$ Th17 cells after secondary culture (Fig. 4*C*, *Left*). Expression of *Rorc* in WT Th17 cells was efficiently maintained, whereas *Rorc* expression in Menin$^{-/-}$ Th17 cells was rapidly lost during extended culture in the absence of IL-6 (second and third cycles, Fig. 4*B*). In addition, the levels of H3-K4Me3 and H3-K9Ac at the *Rorc* gene locus in Menin$^{-/-}$ Th17 cells clearly decreased in

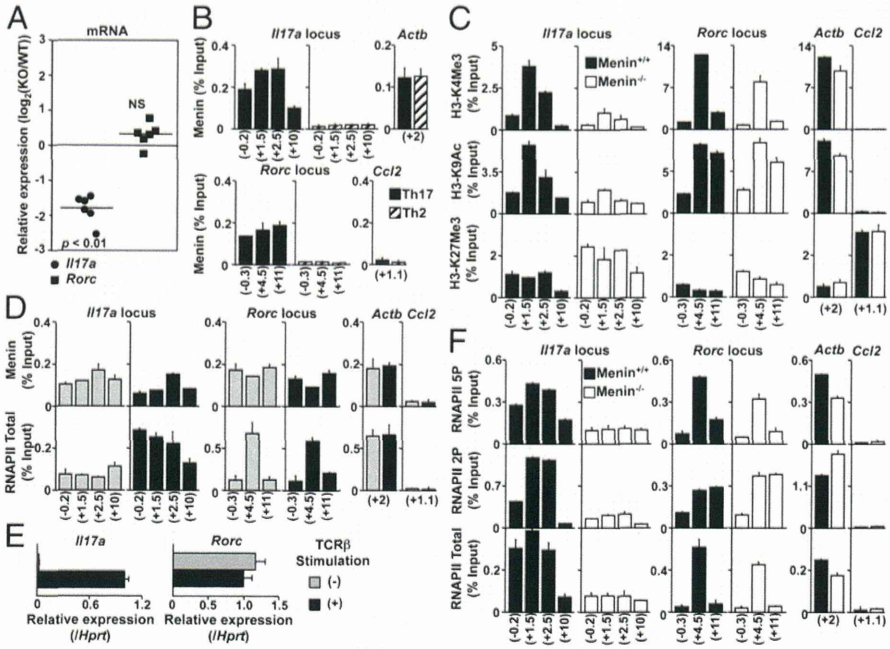

Fig. 3. Menin is required for the formation of permissive histone modifications and RNAPII accumulation at the *Il17a* locus. (*A*) Naive CD4 T cells from WT or Menin-deficient mice were cultured under Th17 conditions for 5 d. Expression of *Il17a* and *Rorc* mRNA were determined by quantitative RT-PCR as described in Fig. 1*A*. Data from six independent experiments with mean values are shown. (*B* and *C*) The binding levels of Menin and RNAPII, and modification of the histone H3-K4Me3, H3-K9Ac, and H3-K27Me3 levels at several regions around the *Il17a*, *Rorc*, *Actb* (active), and *Ccl2* (silent) gene loci were determined by ChIP assays with quantitative PCR (qPCR) analysis. For ChIP with qPCR assay, percentages of input DNA ([specific antibody ChIP – control Ig ChIP]/input DNA; mean of three samples) is shown with SDs. (*D* and *E*) Menin and RNAPII binding or transcripts of the *Il17a* and *Rorc* genes were determined by qPCR in WT Th17 cells stimulated with (+) or without (–) immobilized anti-TCRβ mAb for 4 h. (*F*) RNAPII binding was measured after 4-h restimulation with TCRβ in WT or Menin$^{-/-}$ Th17 cells. Three independent experiments were performed with similar results (*B*–*F*).

the second cycle of culture (Fig. 4*C*, *Middle*). Furthermore, the expression of RORγt protein in Menin$^{-/-}$ Th17 cells was shown to be decreased after the second cycle of cultivation (Fig. 4*D*). Thus, these results indicate that Menin is essential for the maintenance of *Rorc* expression and permissive histone modifications at the *Rorc* gene locus.

Discussion

Previous work has established that the MLL/Menin/TrxG complex plays a critical role in the maintenance of Th2 cell function in murine and human systems (17, 19, 23, 24, 40). We extended this research and herein report a crucial role for Menin in the regulation of Th17 cell differentiation and function. Our results show that Menin bound to the *Il17a* gene locus and induced subsequent histone modifications at the *Il17a* locus together with the expression of *Il17a* in the differentiation phase. Menin was not required for the induction of permissive histone modifications at the *Rorc* gene locus. In sharp contrast to the initial differentiation phase, Menin was required to preserve expression of Rorγt after differentiation. In vivo, Th17 cell-mediated neutrophilic airway inflammation was limited by the abrogation of Menin in Th17 cells, suggesting a physiological role of Menin in the regulation of IL-17–mediated pathology. Thus, these results point to an important role for Menin in the regulation of Th17 cell differentiation and function and also IL-17–dependent pathology.

An interesting finding of the present study is that Menin appeared to function differently at the *Il17a* locus and the *Rorc* locus during the initial Th17 cell differentiation phase. Menin was not required for the induction of permissive histone modifications and transcriptional expression of the *Rorc* locus during Th17 cell differentiation, even though Menin bound strongly to the *Rorc* loci in WT Th17 cells. In the case of Th2 cells, the Menin/TrxG complex did not affect the expression of either the *Gata3* locus or Th2 cytokine loci during the naive to effector Th2 differentiation phase (23). The polycomb protein Ezh2, which can antagonize TrxG function and specifically trimethylate H3K27 to induce repressive histone modifications, appears to regulate effector Th1/Th2 cell differentiation primarily via control of the expression of lineage-specific transcription factor genes rather than the cytokine genes (18). Although the underlying mechanisms that determine which genes the TrxG and PcG complexes functionally target remain unclear, the binding of these chromatin-modifying complexes alone does not always correlate with the expected modification of histones or transcription. Our preliminary results indicate that the *Il17f* locus behaves in a similar fashion to the *Rorc* locus in terms of the binding of Menin and the state of histone modifications, i.e., Menin was not required for the induction of *Il17f* expression and permissive histone modifications in differentiating Th17 cells.

In contrast to the initial induction phase of Th17 cell differentiation, the Menin/TrxG complex plays a crucial role in the maintenance of *Rorc* expression and permissive histone modifications that are required to support appropriate function of Th17 cells. Indeed, IL-6 is required for the induction of Th17 cell differentiation but not for the maintenance of Th17 function (39), indicating that the underlying mechanisms governing the expression of *Rorc* and *Il17a* are likely to be different between the differentiation and maintenance phases. Our previous report showed that the Menin/TrxG complex is essential to retain *Gata3* expression after differentiation, whereas IL-4–mediated STAT6 activation is dispensable (23). GATA3 expression is required for the maintenance of Th2 cell function during long-term culture (23) and also during the memory phase in both mouse and human systems (24, 41). Our finding that STAT3 deficiency in Th17 cells results in impaired Menin binding to the *Il17a* and *Rorc* loci, indicates that STAT3 and TGF-β–mediated recruitment of Menin is likely an important mechanism in the induction of permissive histone modifications at these genes in differentiating Th17 cells.

It has been reported that the Menin/TrxG complex binds to DNA through RNAPII (22, 40). We demonstrate that Menin directly bound to the *Il17a* gene locus and induced permissive histone modifications in differentiating Th17 cells (Fig. 3 and Fig. S4). Menin may bind to DNA through low levels of RNAPII bound to the *Il17a* gene locus in differentiating Th17 cells. However, we also found that Menin is required for TCR restimulation-induced RNAPII recruitment and Ser-2/Ser-5 double phosphorylation of RNAPII at the *Il17a* gene locus that accompanies the dramatic induction of *Il17a* expression after TCR restimulation (Fig. 3*E*). This reveals a previously unidentified unexpected mechanism for the Menin/TrxG complex in the regulation of gene expression, i.e., Menin is essential for rapid recruitment of the RNAPII transcription complex and high-level transcription of target genes such as *Il17a*. The sequential recruitment of the Menin/TrxG complex and the RNAPII transcription complex appears to be important to establish a fully active transcriptional state capable of rapidly inducing target gene expression after exposure to an external stimuli such as TCR stimulation. It will thus be important to determine to what extent Menin retains this function as a facilitator of RNAPII recruitment at other genes and in other cell types.

We found that Th17 cell-mediated neutrophilic airway inflammation is markedly attenuated in the mice transferred with Menin$^{-/-}$ Th17 cells and CD4-Cre^{+}Menin$^{fl/fl}$ mice (Fig. 2). The dramatic effect observed in these experimental settings may reflect the decreased numbers of IL-17A–producing cells and also the impaired maintenance of Th17 cell function of the Menin$^{-/-}$ Th17 cells. Noneosinophilic asthma associated with neutrophilic inflammation is generally refractive to treatment with steroids

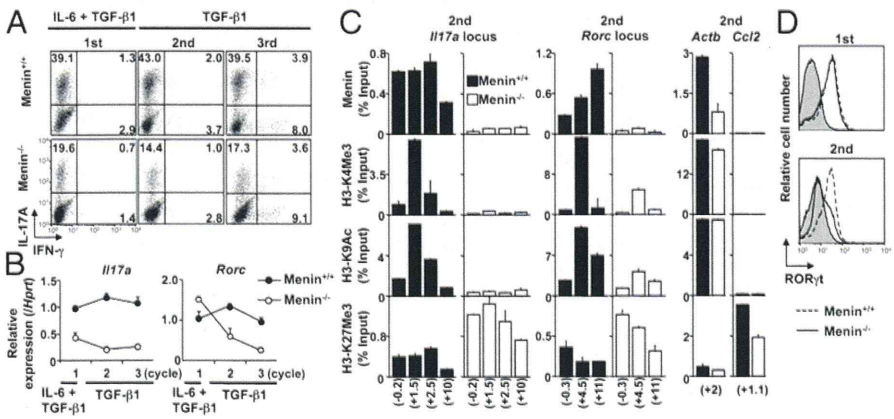

Fig. 4. Menin$^{-/-}$ Th17 cells fail to maintain the expression of *Rorc*. (*A* and *B*) Th17 cells (first, second, and third cycle) were generated as described in *Materials and Methods*. IL-17A– and IFN-γ–secreting cells were assessed by FACS (*A*), and *Il17a* and *Rorc* mRNA expression were determined by quantitative RT-PCR (*B*). Four independent experiments were performed with similar results (*A* and *B*). Mean values with SDs ($n = 3$) are shown (*A*). (*C*) The binding of Menin and levels of histone modifications after the second culture cycle at the indicated gene loci were determined by ChIP assays with qPCR as described in Fig. 3*B*. (*D*) The level of RORγt protein expression were determined by FACS. Data are representative of two independent experiments (*C* and *D*).

(42, 43). Multiple mechanisms have been identified by which Th17 cells can cause steroid-resistant asthma (44). It is recognized that IL-17 family members induce granulopoiesis, neutrophil chemotaxis, and the antiapoptotic properties of G-CSF (45, 46). Our study revealed that neutrophilic airway inflammation induced by Th17 cells was attenuated in the mice transferred with Menin$^{-/-}$ Th17 cells and CD4-Cre^{+}Menin$^{fl/fl}$ mice. Menin may also play an important role in some types of neutrophilic airway inflammation in humans.

In summary, our study highlights that Menin regulates both the induction and maintenance of Th17 differentiation and function in vitro, and contributes IL-17–mediated pathogenicity in vivo. Thus, the components of Menin/TrxG complex could represent unique therapeutic targets for the treatment of Th17 cell–mediated steroid-resistant asthma in humans.

Materials and Methods

C57BL/6 and BALB/c mice were purchased from CLEA. Menin$^{fl/fl}$ mice (47) were purchased from The Jackson Laboratory and backcrossed at Chiba University to C57BL/6 or BALB/c background more than 10 times. CD4-Cre Transgenic mice were purchased from Taconic Farms. STAT3$^{fl/fl}$ mice were provided by T. Hirano (Osaka University, Osaka) (48). All mice used in this study were maintained under specific pathogen-free conditions and ranged from 6 to 8 wk of age. All animal care was performed in accordance with the guidelines of Committee on the Ethics of Animal Experiments of Chiba University.

Detailed descriptions of all materials and methods are provided in *SI Materials and Methods*.

ACKNOWLEDGMENTS. We thank Kaoru Sugaya, Hikari Kato, Miki Kato, and Toshihiro Ito for their excellent technical assistance. This work was supported by the Global Centers of Excellence Program (Global Center for Education and Research in Immune System Regulation and Treatment), and by grants from the Ministry of Education, Culture, Sports, Science and Technology [Grants-in-Aid for Scientific Research (S) 26221305; (C) 24592083; Young Scientists (B) 22790452, 25860351, and 25860352; Research Activity Start-up 25893032 and 25893033], the Ministry of Health, Labour and Welfare, the Astellas Foundation for Research on Metabolic Disorders, the Uehara Memorial Foundation, Osaka Foundation for Promotion of Fundamental Medical Research, Princes Takamatsu Cancer Research Fund, and Takeda Science Foundation. D.J.T. was supported by Japanese Society for the Promotion of Science Postdoctoral Fellowship 2109747.

1. Reiner SL (2007) Development in motion: Helper T cells at work. *Cell* 129(1):33–36.
2. O'Shea JJ, Paul WE (2010) Mechanisms underlying lineage commitment and plasticity of helper CD4^{+} T cells. *Science* 327(5969):1098–1102.
3. Szabo SJ, et al. (2000) A novel transcription factor, T-bet, directs Th1 lineage commitment. *Cell* 100(6):655–669.
4. Zheng W, Flavell RA (1997) The transcription factor GATA-3 is necessary and sufficient for Th2 cytokine gene expression in CD4 T cells. *Cell* 89(4):587–596.
5. Löhning M, Richter A, Radbruch A (2002) Cytokine memory of T helper lymphocytes. *Adv Immunol* 80:115–181.
6. Ansel KM, Djuretic I, Tanasa B, Rao A (2006) Regulation of Th2 differentiation and Il4 locus accessibility. *Annu Rev Immunol* 24:607–656.
7. Harrington LE, et al. (2005) Interleukin 17-producing CD4^{+} effector T cells develop via a lineage distinct from the T helper type 1 and 2 lineages. *Nat Immunol* 6(11): 1123–1132.
8. Park H, et al. (2005) A distinct lineage of CD4 T cells regulates tissue inflammation by producing interleukin 17. *Nat Immunol* 6(11):1133–1141.
9. Bettelli E, et al. (2006) Reciprocal developmental pathways for the generation of pathogenic effector TH17 and regulatory T cells. *Nature* 441(7090):235–238.
10. Ivanov II, et al. (2006) The orphan nuclear receptor RORgammat directs the differentiation program of proinflammatory IL-17^{+} T helper cells. *Cell* 126(6):1121–1133.
11. Stockinger B, Veldhoen M, Martin B (2007) Th17 T cells: Linking innate and adaptive immunity. *Semin Immunol* 19(6):353–361.
12. Leonardi C, et al. (2012) Anti-interleukin-17 monoclonal antibody ixekizumab in chronic plaque psoriasis. *N Engl J Med* 366(13):1190–1199.
13. Molet S, et al. (2001) IL-17 is increased in asthmatic airways and induces human bronchial fibroblasts to produce cytokines. *J Allergy Clin Immunol* 108(3):430–438.
14. Allan RS, et al. (2012) An epigenetic silencing pathway controlling T helper 2 cell lineage commitment. *Nature* 487(7406):249–253.
15. Kanno Y, Vahedi G, Hirahara K, Singleton K, O'Shea JJ (2012) Transcriptional and epigenetic control of T helper cell specification: Molecular mechanisms underlying commitment and plasticity. *Annu Rev Immunol* 30:707–731.
16. Schuettengruber B, Chourrout D, Vervoort M, Leblanc B, Cavalli G (2007) Genome regulation by polycomb and trithorax proteins. *Cell* 128(4):735–745.
17. Nakayama T, Yamashita M (2009) Critical role of the Polycomb and Trithorax complexes in the maintenance of CD4 T cell memory. *Semin Immunol* 21(2):78–83.
18. Tumes DJ, et al. (2013) The polycomb protein Ezh2 regulates differentiation and plasticity of CD4^{+} T helper type 1 and type 2 cells. *Immunity* 39(5):819–832.
19. Yamashita M, et al. (2006) Crucial role of MLL for the maintenance of memory T helper type 2 cell responses. *Immunity* 24(5):611–622.
20. Milne TA, et al. (2002) MLL targets SET domain methyltransferase activity to Hox gene promoters. *Mol Cell* 10(5):1107–1117.
21. Chandrasekharappa SC, et al. (1997) Positional cloning of the gene for multiple endocrine neoplasia-type 1. *Science* 276(5311):404–407.
22. Yokoyama A, et al. (2005) The menin tumor suppressor protein is an essential oncogenic cofactor for MLL-associated leukemogenesis. *Cell* 123(2):207–218.
23. Onodera A, et al. (2010) STAT6-mediated displacement of polycomb by trithorax complex establishes long-term maintenance of GATA3 expression in T helper type 2 cells. *J Exp Med* 207(11):2493–2506.
24. Nakata Y, et al. (2010) c-Myb, Menin, GATA-3, and MLL form a dynamic transcription complex that plays a pivotal role in human T helper type 2 cell development. *Blood* 116(8):1280–1290.
25. Guru SC, et al. (1998) Identification and characterization of the multiple endocrine neoplasia type 1 (MEN1) gene. *J Intern Med* 243(6):433–439.
26. Acosta-Rodriguez EV, Napolitani G, Lanzavecchia A, Sallusto F (2007) Interleukins 1beta and 6 but not transforming growth factor-beta are essential for the differentiation of interleukin 17-producing human T helper cells. *Nat Immunol* 8(9):942–949.
27. Ghoreschi K, et al. (2010) Generation of pathogenic T_H17 cells in the absence of TGF-β signalling. *Nature* 467(7318):967–971.
28. Iezzi G, et al. (2009) CD40-CD40L cross-talk integrates strong antigenic signals and microbial stimuli to induce development of IL-17-producing CD4^{+} T cells. *Proc Natl Acad Sci USA* 106(3):876–881.
29. Gomez-Rodriguez J, et al. (2009) Differential expression of interleukin-17A and -17F is coupled to T cell receptor signaling via inducible T cell kinase. *Immunity* 31(4): 587–597.
30. Al-Ramli W, et al. (2009) T(H)17-associated cytokines (IL-17A and IL-17F) in severe asthma. *J Allergy Clin Immunol* 123(5):1185–1187.
31. McKinley L, et al. (2008) TH17 cells mediate steroid-resistant airway inflammation and airway hyperresponsiveness in mice. *J Immunol* 181(6):4089–4097.
32. Ito K, et al. (2008) Steroid-resistant neutrophilic inflammation in a mouse model of an acute exacerbation of asthma. *Am J Respir Cell Mol Biol* 39(5):543–550.
33. Hirahara K, et al. (2010) Signal transduction pathways and transcriptional regulation in Th17 cell differentiation. *Cytokine Growth Factor Rev* 21(6):425–434.
34. Hughes CM, et al. (2004) Menin associates with a trithorax family histone methyltransferase complex and with the hoxc8 locus. *Mol Cell* 13(4):587–597.
35. Orphanides G, Reinberg D (2002) A unified theory of gene expression. *Cell* 108(4): 439–451.
36. Czudnochowski N, Bösken CA, Geyer M (2012) Serine-7 but not serine-5 phosphorylation primes RNA polymerase II CTD for P-TEFb recognition. *Nat Commun* 3:842.
37. Durant L, et al. (2010) Diverse targets of the transcription factor STAT3 contribute to T cell pathogenicity and homeostasis. *Immunity* 32(5):605–615.
38. Yang XP, et al. (2011) Opposing regulation of the locus encoding IL-17 through direct, reciprocal actions of STAT3 and STAT5. *Nat Immunol* 12(3):247–254.
39. Lee YK, et al. (2009) Late developmental plasticity in the T helper 17 lineage. *Immunity* 30(1):92–107.
40. Nakayama T, Yamashita M (2008) Initiation and maintenance of Th2 cell identity. *Curr Opin Immunol* 20(3):265–271.
41. Endo Y, et al. (2011) Eomesodermin controls interleukin-5 production in memory T helper 2 cells through inhibition of activity of the transcription factor GATA3. *Immunity* 35(5):733–745.
42. Pavord ID, Brightling CE, Woltmann G, Wardlaw AJ (1999) Non-eosinophilic corticosteroid unresponsive asthma. *Lancet* 353(9171):2213–2214.
43. Pavord ID (2007) Non-eosinophilic asthma and the innate immune response. *Thorax* 62(3):193–194.
44. Alcorn JF, Crowe CR, Kolls JK (2010) TH17 cells in asthma and COPD. *Annu Rev Physiol* 72:495–516.
45. Kolls JK, Lindén A (2004) Interleukin-17 family members and inflammation. *Immunity* 21(4):467–476.
46. Ouyang W, Kolls JK, Zheng Y (2008) The biological functions of T helper 17 cell effector cytokines in inflammation. *Immunity* 28(4):454–467.
47. Crabtree JS, et al. (2003) Of mice and MEN1: Insulinomas in a conditional mouse knockout. *Mol Cell Biol* 23(17):6075–6085.
48. Takeda K, et al. (1998) Stat3 activation is responsible for IL-6-dependent T cell proliferation through preventing apoptosis: Generation and characterization of T cell-specific Stat3-deficient mice. *J Immunol* 161(9):4652–4660.

Sasahara et al. Radiation Oncology 2014, 9:92
http://www.ro-journal.com/content/9/1/92

RADIATION ONCOLOGY

RESEARCH Open Access

Effects of the dose-volume relationship on and risk factors for maxillary osteoradionecrosis after carbon ion radiotherapy

Go Sasahara[1], Masashi Koto[2*], Hiroaki Ikawa[2], Azusa Hasegawa[2], Ryo Takagi[2], Yoshitaka Okamoto[1] and Tadashi Kamada[2]

Abstract

Background: Osteoradionecrosis (ORN) is a critical complication after carbon ion (C-ion) or photon radiotherapy (RT) for head and neck tumors. However, the risk factors for ORN after C-ion RT remain unclear. Therefore, the present study aimed to investigate the effects of the dose-volume relationship on and risk factors for ORN development after C-ion RT. We, however, focused on the maxillary bone because most tumors treated with C-ion RT were primarily located in the sinonasal cavity.

Methods: The patients enrolled in this study received more than 10% of the prescribed total dose of 57.6 Gy equivalent (GyE) in 16 fractions to their maxilla. All patients were followed up for more than 2 years after C-ion RT. Those with tumor invasion to the maxilla before C-ion RT or local recurrence after the treatment were excluded from the study to accurately evaluate the effects of irradiation on the bone. Sixty-three patients were finally selected. The severity of ORN was assessed according to the Common Terminology Criteria for Adverse Events version 4.0. The correlation between clinical and dosimetric parameters and ORN incidence was retrospectively analyzed.

Results: The median follow-up period was 79 months. Of the 63 enrolled patients, 26 developed ORN of grade ≥1. Multivariate analysis revealed that the maxilla volume receiving more than 50 GyE (V50) and the presence of teeth within the planning target volume were significant risk factors for ORN. Dose-volume histogram analysis revealed that V10 to V50 parameters were significantly higher in patients with ORN than in those without ORN.

Conclusions: V50 and the presence of teeth within the planning target volume were independent risk factors for the development of ORN after C-ion RT using a 16-fraction protocol.

Keywords: Carbon ion radiotherapy, Osteoradionecrosis, Head and neck tumor, Dose-volume histogram

Background

Carbon ion radiotherapy (C-ion RT) offers a potential cure for radio-resistant tumors owing to its increased biologic potential and improved dose localization properties. In a recent report, we demonstrated that C-ion RT was a promising treatment option for various inoperable and radio-resistant tumors [1].

In addition, we have published the results of a phase II clinical trial of C-ion RT in patients with head and neck tumors [2]. In this trial, C-ion RT demonstrated excellent disease control in radio-resistant tumors such as mucosal malignant melanoma, adenoid cystic carcinoma, and adenocarcinoma. However, the development of osteoradionecrosis (ORN) remained one of the serious complications after C-ion RT.

ORN is a well-documented complication of photon RT for head and neck tumors. The degree of ORN varies from limited, asymptomatic bone exposures that may remain stable for a prolonged period of time or heal with conservative management, to severe necroses necessitating surgical intervention and reconstruction [3]. Thus, ORN is a serious clinical problem. Several clinical risk factors for ORN such as smoking, drinking, oral hygiene, and tumor characteristics have been implicated in the literature [3-5].

* Correspondence: koto@nirs.go.jp
[2]Research Center for Charged Particle Therapy Hospital, National Institute of Radiological Sciences, Chiba, Japan
Full list of author information is available at the end of the article

The radiation dose or dose-volume histogram (DVH) parameter has been also known to be a major contributor to ORN [4,6-9]. However, there remains a lack of data on ORN after C-ion RT.

The present study aimed to investigate the effects of the dose-volume relationship on and risk factors for ORN development after C-ion RT. We, however, focused on the maxillary bone in this investigation because most tumors treated with C-ion RT were located in the sinonasal cavity.

Methods

Patients and tumor characteristics

From April 1997 to February 2006, a total of 236 patients with head and neck tumors were treated with C-ion RT in a phase II clinical trial at our institution [2]. Of these, patients who received more than 10% of a prescribed total dose of 57.6 gray equivalent (GyE) in 16 fractions to the maxilla and were followed up for more than 2 years after C-ion RT were selected. Those with tumor invasion to the maxilla before C-ion RT or local recurrence after treatment were excluded from the study to accurately evaluate the effects of irradiation on the maxilla. Based on results from a previous clinical trial [10], a total dose of 57.6 GyE or 64.0 GyE in 16 fractions was prescribed for head and neck tumors. However, only patients treated with 57.6 GyE were included in the present study as a homogeneous population for analysis. Sixty-three patients were finally included in our study cohort.

Before C-ion RT, all patients provided written informed consent acknowledging the possibility of ORN as a result of the treatment. The study was approved by the institutional ethics committee (National Institute of Radiological Sciences).

The median age of the 63 enrolled patients (32 men and 31 women) was 59 years (range, 16–80 years). Of these, 22 smoked and 31 consumed alcohol. The presence of teeth within the planning target volume (PTV) was documented in 29 patients. Histological classification of all patients' tumors included 24 patients of malignant melanoma, 24 adenoid cystic carcinomas, 9 adenocarcinomas, 2 squamous cell carcinomas, 2 mucoepidermoid carcinomas, and 1 each of epithelial/myoepithelial carcinoma and undifferentiated carcinoma. Eighteen of the studied tumors were located in the paranasal sinus, 17 in the nasal cavity, 12 on the parotid gland, 6 in the oral cavity, and 10 at other sites. All patients underwent dental examination and management before C-ion RT. If dental extraction was necessary, C-ion RT was performed at least 10 days after such procedure. Of the 23 patients who received adjuvant or neo-adjuvant chemotherapy, 18 had malignant mucosal melanoma and received combinatorial chemotherapy with dacarbazine, nimustine, and vincristine.

C-ion RT

For C-ion RT, each patient was positioned in customized cradles (Moldcare; Alcare, Tokyo, Japan) and immobilized with a low-temperature thermoplastic device (Shellfitter; Kuraray, Osaka, Japan). A set of computed tomography (CT) images at 2.5-mm slide thickness was obtained for treatment planning using the immobilization devices. Three-dimensional treatment planning was performed with HIPLAN software [11].

The clinical target volume had a minimum margin of 5 mm added to the gross tumor volume. Furthermore, a margin of 3–5 mm was added as an internal and setup margin around the clinical target volume to create a final PTV. In principle, more than 3 portals were used to improve dose distribution.

During each treatment session, the patient's position was verified with a computer-aided online positioning system. The patient was positioned on the treatment couch using immobilization devices, and then digital orthogonal radiographic images were taken and transferred to the positioning computer. The positioning images were compared with the reference images digitally reconstructed from CT scans. If the difference in positioning was more than 2 mm, the treatment couch was repositioned until appropriate.

The carbon beam dose was expressed in terms of photon equivalent dose, defined as the physical dose multiplied by the relative biological effectiveness (RBE) of carbon ions. The clinical RBE of the carbon beam at our institute was determined according to the RBE for acute skin reaction, which was 3.0 at the distal part of the spread-out Bragg peak [12]. C-ion RT was delivered in 16 fractions over a 4-week period with 4 treatment days per week. The prescribed total dose was 57.6 GyE in all patients. C-ion RT was performed without concurrent chemotherapy in all patients.

Follow-up and ORN evaluation

After C-ion RT, patients were followed up every 2 to 3 months during the first 2 years and every 3 to 6 months thereafter. Magnetic resonance imaging (MRI) examination of the head and neck region was performed at 4–6-month intervals. A diagnosis of maxillary ORN was indicated on the basis of clinical symptoms, macroscopic observation, and MRI findings demonstrating an area of low intensity on T1-weighted images and/or that of high-intensity on T2-weighted images present within the irradiation field after C-ion RT (Figure 1). Enhancement on post-contrast images and diffusion-weighted images were used to exclude the possibility of local recurrence. The severity of ORN was assessed according to the Common Terminology Criteria for Adverse Events version 4.0 as follows: grade 1, asymptomatic with clinical or diagnostic observations only and intervention not indicated; grade 2,

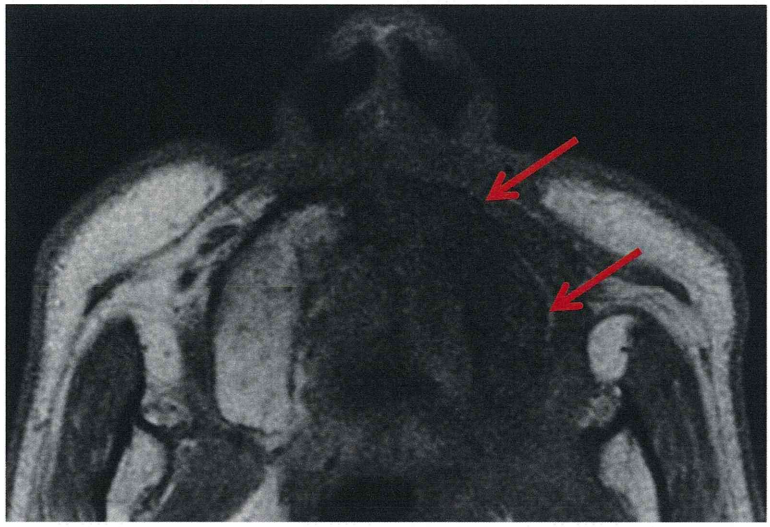

Figure 1 Representative magnetic resonance image (MRI) of the maxillary osteoradionecrosis. T1-weighted axial MRI showed low signal appearance in the left maxilla (red arrows).

symptomatic, limiting instrumental activities of daily living, and medical intervention indicated; grade 3, severe symptoms, limiting self-care activities of daily living, and selective surgical intervention indicated; grade 4, life-threatening consequences with urgent intervention indicated. The highest grade was used for analysis.

Dose-volume histogram analysis

DVH analysis was performed to identify the dose-volume effects on and risk factors for maxillary ORN. The maxillary DVH included the alveolar process and palatine process of the maxilla. However, the pterygoid process and maxillary sinus were not included. Additionally, the root portion of each tooth embedded in the maxilla was included, but its crown was not (Figure 2). Cumulative DVH of the maxilla was calculated during treatment planning. Based on the DVH data obtained from HIPLAN software, the maxilla volumes receiving more than 10–50 GyE in 10-GyE increments were expressed as DVH parameters V10–50 (ml). The average volume of the maxilla was 27.0 ml (range, 12.5–49.8 ml).

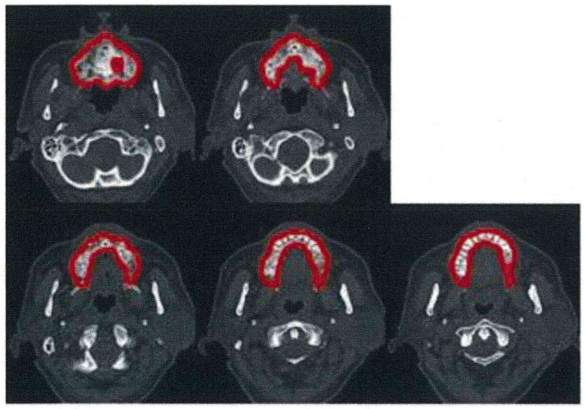

Figure 2 Representative contouring of the maxilla. All computed tomography images of the contoured maxilla are shown.

Statistical analysis

The follow-up time was calculated from the first date of irradiation. On univariate analysis of different subgroups, cumulative incidence of maxillary ORN was evaluated using the Kaplan–Meier method and compared by the log-rank test. Furthermore, factors with statistical significance on univariate analysis were applied to multivariate analysis using Cox's proportional hazard model. To compare the irradiated maxilla volumes, the Mann-Whitney U test was used. A p value of <0.05 was considered statistically significant. All statistical analysis was performed using the SPSS software version 11 (SPSS Inc., Chicago, IL).

Results

Incidence of maxillary ORN

The median follow-up time was 79 months (range, 24–167 months). Of the 63 enrolled patients, maxillary ORN developed in 26 (41.3%). The median interval between treatment initiation and maximum ORN observation was 23 months (range, 6–107 months). Grade 1 ORN was observed in 14 patients; grade 2, in 9, and grade 3, in 3. None of the patients experienced grade 4 ORN. The 3 patients with grade 3 ORN underwent sequestrectomy for pain control. Subsequently, they also received implantation of a denture and palatal prosthesis.

Risk factors for maxillary ORN

Univariate analysis was performed for clinical and DVH parameters to analyze their effects on the development of grade ≥1 ORN (Table 1). Patients were divided into 2 groups by median values for analysis of both age and DVH parameters. On univariate analysis, large V10 to V50 values, chemotherapy, and the presence of teeth within the PTV were found to correlate with ORN development. However, factors such as age, sex, smoking, and alcohol consumption had no influence on ORN occurrence.

Multivariate analysis was performed with the factors that reached statistical significance on univariate analysis: V10 to V50 values, chemotherapy, and the presence of teeth within the PTV. All data on DVH parameters were evaluated as continuous variables, as opposed to discrete cutoff points used in univariate analysis. Multivariate analysis revealed that V50 ($p = 0.0009$; hazard ratio [HR] = 1.15; 95% confidence interval [CI] = 1.06–1.25) and the presence of teeth within the PTV ($p = 0.0001$; HR = 11.3; 95% CI = 3.25–39.35) were significant independent risk factors for ORN (Table 2).

Table 1 Univariate analysis of risk factors of osteoradionecrosis

Factors	Subgroup	n	p value	5-y ORN rate (%)
V10	<14.5 ml	31		26.1
	≥14.5 ml	32	0.015	53
V20	<11.9 ml	31		20
	≥11.9 ml	32	0.001	58.5
V30	<8.1 ml	31		13.7
	≥8.1 ml	32	0.001	64.4
V40	<4.6 ml	31		12.1
	≥4.6 ml	32	0.0002	67.7
V50	<3.0 ml	31		11.7
	≥3.0 ml	32	0.0002	69.5
Age (years)	<59	31		33.5
	≥59	32	0.23	45.5
Sex	Male	31		40.4
	Female	32	0.5	38.2
Teeth in the PTV	None	34		5.9
	Some	29	0.0001	81
Smoking	Yes	22		41.6
	No	41	0.66	38.6
Alcohol	Yes	31		48.6
	No	32	0.11	30.3
Chemotherapy	Yes	23		54.0
	No	40	0.04	30.5

A large V10 to V50 and the presence of teeth within the PTV were found to correlate with ORN development.

Table 2 Multivariate analysis of risk factors of osteoradionecrosis

	Hazard ratio	95% confidence interval	p value
V50	1.15	1.06–1.25	0.0009
Teeth in the PTV	11.3	3.25–39.35	0.0001

V50 and the presence of teeth within the PTV were significant independent risk factors for ORN.

Correlation between DVH parameters and ORN

Figure 3 shows the mean percentages of DVH parameters from V10 to V50 in patients with and without ORN. All DVH parameters were significantly higher in patients with ORN than in those without ORN (Table 3).

Discussion

ORN of the maxilla is a serious adverse event in patients receiving C-ion RT for head and neck tumors. Therefore, it is clinically important to define the risk factors for ORN. In the present study, we demonstrated that ORN development after C-ion RT correlated with dosimetric parameters. In addition, our results confirmed that V50 and the presence of teeth within the PTV were independent risk factors for ORN.

Several previous studies have reported the effects of dosimetric parameters on ORN prediction [4,6-8]. Tsai *et al.* [6] reviewed 402 oropharyngeal cancer patients treated with definitive photon RT using three-dimensional conformal radiotherapy or intensity modulated radiotherapy for ORN and revealed that V40, V50, and V60 were risk factors for ORN on univariate analysis, whereas V50 and V60 were also risk factors on multivariate analysis. On the basis of such findings, they concluded that minimizing the percentage of bone volume exposed to 50 Gy could reduce ORN risk. In our study, although a 16-fraction protocol was used for C-ion RT, V50 remained a statistically significant independent risk factor for ORN. If the predetermined RBE value was correct, and the linear-quadratic model could be applied to C-ion RT, 50 GyE in 16 fractions would be equivalent to 61.1 GyE at a standard fractionation of 2 GyE per fraction with a 3-Gy α/β value.

Chang *et al.* [7] reported that a radiation dose of more than 70 Gy was associated with an increased risk for ORN. Ben-David *et al.* [4] and Studer *et al.* [8] suggested that ORN might be related to mandibular volumes receiving high doses as the situation could exacerbate bone exposure caused by severe acute mucositis. Therefore, a reduction of the bone volume exposed to a high radiation dose may prevent ORN. When comparing the DVH parameters between patients with ORN and those without, a significant difference was observed even at lower radiation doses. However, the effects of low radiation dose on the occurrence of ORN remain unclear. In the above-mentioned study by Tsai *et al.* [6], V10 to V30 were not risk factors for ORN on univariate analysis. In

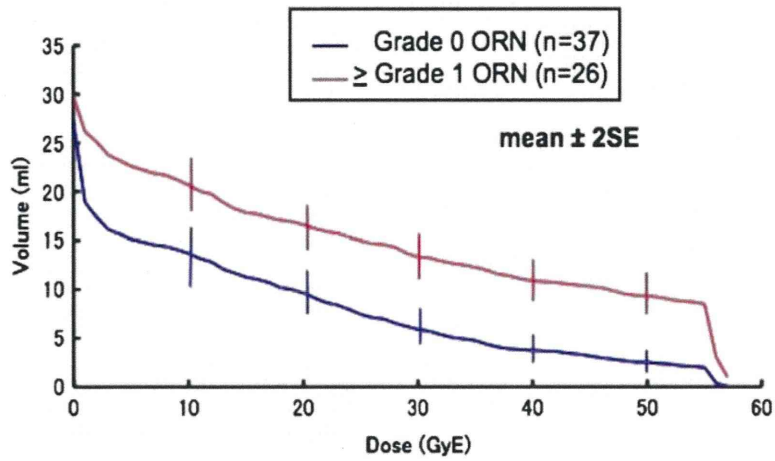

Figure 3 The average maxillary volumes receiving 10 to 50 GyE according to the occurrence of osteoradionecrosis. All DVH parameters were significantly higher in patients with ORN than in those without.

our study, however, all DVH parameters including V10 to V30 were risk factors for ORN on univariate analysis, although only V50 was confirmed as a risk factor by multivariate analysis. The difference between C-ion RT and photon RT data for low doses might result from dose distribution features of these modalities. In three-dimensional conformal radiotherapy and intensity modulated radiotherapy, low-dose regions are generally enlarged because multi-portals are used to ensure conformable dose distribution to the target. On the other hand, C-ion RT can deliver conformable dose distribution to the target without expanding the low-dose regions [13]. Therefore, the maxilla volumes irradiated at low doses in C-ion RT might actually correlate with those receiving higher doses.

In our study, the presence of teeth within the PTV was indicated as an independent risk factor for ORN after C-ion RT. The correlation between the presence of teeth within the PTV and ORN in photon RT has also been reported. Morrish *et al.* [14] reported that ORN developed in 19 of 78 (24.4%) patients with in-field teeth, whereas only 3 of 22 (13.6%) patients without in-field teeth experienced the condition. Additionally, Chang *et al.* [7] reported that the rate of ORN for patients with in-field teeth was 32/239 (13.4%), while it was only 5/174 (2.9%) for those without in-field teeth. ORN has been suggested to develop as a result of gingiva regression by irradiation, leading to an environment that is susceptible to bone infection [15]. In fact, ORN development was found around the tooth in several patients after C-ion RT. Thus, oral care after treatment is very important, especially in cases when teeth are included in the PTV.

Table 3 Correlation between dose-volume histogram parameters and osteoradionecrosis

Parameters (mean, ml)	ORN	No ORN	p value
V10	20.68	13.71	0.0054
V20	16.55	9.64	0.0004
V30	13.34	5.86	<0.0001
V40	10.90	3.73	<0.0001
V50	9.32	2.48	<0.0001

All DVH parameters were significantly higher in patients with ORN than in those without ORN.

Most available reports on ORN after photon RT to head and neck tumors have focused on the mandible. In the present study, we instead investigated ORN of the maxilla because tumors treated with C-ion RT were primarily located in the sinonasal cavity. However, our results on ORN of the maxilla were similar to previous findings on the mandible. Although the mandible is also irradiated in C-ion RT for sinonasal tumors, the radiation dose delivered to the mandible could be reduced owing to its superior physical spatial distribution.

In our study, ORN was observed on the basis of MRI findings in 26 of 63 patients (41.3%) during a median follow-up time of 79 months. Owing to the sensitivity of MRI, 14 of the 26 patients were diagnosed with grade 1 ORN and exhibited no clinical symptoms. Grade 3 ORN was observed in only 3 patients.

Since the present study aimed to investigate the effects of irradiation on ORN development in patients treated with C-ion RT, patients with tumor invasion to the maxilla before C-ion RT were excluded, as it may be challenging to distinguish between osteomyelitis caused by tumor invasion and ORN.

Conclusion

Our findings from the present study are useful for predicting the risk of ORN and therefore preventing the development of such a condition after C-ion RT for head and neck tumors. We found that ORN development

after C-ion RT was correlated with dosimetric parameters. In addition, V50 and the presence of teeth within the PTV were risk factors for the development of ORN after C-ion RT. Such findings confirmed the dose-volume effects on ORN development.

Abbreviations

C-ion RT: Carbon ion radiotherapy; ORN: Osteoradionecrosis; DVH: Dose-volume histogram; GyE: Gray equivalent; PTV: Planning target volume; CT: Computed tomography; RBE: Relative biological effectiveness; MRI: Magnetic resonance imaging; V10-50: Maxilla volumes receiving more than 10–50 GyE; n: Number.

Competing interests

The authors declare that they have no competing interests.

Authors' contributions

MK and AH conceived the study. GS, HI, and RT participated in data collection. GS performed statistical analysis and drafted the manuscript. MK helped drafting the manuscript. TK and YO critically reviewed the manuscript. All authors read and approved the final manuscript.

Author details

[1]Department of Otorhinolaryngology, Head and Neck Surgery, Chiba University Graduate School of Medicine, Chiba, Japan. [2]Research Center for Charged Particle Therapy Hospital, National Institute of Radiological Sciences, Chiba, Japan.

Received: 15 December 2013 Accepted: 29 March 2014
Published: 3 April 2014

References

1. Tsujii H, Kamada T: **A review of update clinical results of carbon ion radiotherapy.** *Jpn J Clin Oncol* 2012, **42**:670–685.
2. Mizoe JE, Hasegawa A, Jingu K, Takagi R, Bessyo H, Morikawa T, Tonoki M, Tsuji H, Kamada T, Tsujii H, Okamoto Y, Organizing Committee for the Working Group for Head Neck Cancer: **Results of carbon ion radiotherapy for head and neck cancer.** *Radiother Oncol* 2012, **103**:32–37.
3. Mendenhall WM: **Mandibular osteoradionecrosis.** *J Clin Oncol* 2004, **22**:4867–4868.
4. Ben-David MA, Diamante M, Radawski JD, Vineberg KA, Stroup C, Murdoch-Kinch CA, Zwetchkenbaum SR, Eisbruch A: **Lack of osteoradionecrosis of the mandible after intensity-modulated radiotherapy for head and neck cancer: likely contributions of both dental care and improved dose distributions.** *Int J Radiat Oncol Biol Phys* 2007, **68**:396–402.
5. Wang X, Hu C, Eisbruch A: **Organ-sparing radiation therapy for head and neck cancer.** *Nat Rev Clin Oncol* 2011, **8**:639–648.
6. Tsai CJ, Hofstede TM, Sturgis EM, Garden AS, Lindberg ME, Wei Q, Tucker SL, Dong L: **Osteoradionecrosis and radiation dose to the mandible in patients with oropharyngeal cancer.** *Int J Radiat Oncol Biol Phys* 2013, **85**:415–420.
7. Chang DT, Sandow PR, Morris CG, Hollander R, Scarborough L, Amdur RJ, Mendenhall WM: **Do pre-irradiation dental extractions reduce the risk of osteoradionecrosis of the mandible?** *Head Neck* 2007, **29**:528–536.
8. Studer G, Studer SP, Zwahlen RA, Huguenin P, Grätz KW, Lütolf UM, Glanzmann C: **Osteoradionecrosis of the mandible: minimized risk profile following intensity-modulated radiation therapy (IMRT).** *Strahlenther Onkol* 2006, **182**:283–288.
9. Lee IJ, Koom WS, Lee CG, Kim YB, Yoo SW, Keum KC, Kim GE, Choi EC, Cha IH: **Risk factors and dose-effect relationship for mandibular osteoradionecrosis in oral and oropharyngeal cancer patients.** *Int J Radiat Oncol Biol Phys* 2009, **75**:1084–1091.
10. Mizoe JE, Tsujii H, Kamada T, Matsuoka Y, Tsuji H, Osaka Y, Hasegawa A, Yamamoto N, Ebihara S, Konno A: **Organizing Committee for the Working Group for Head-And-Neck Cancer: Dose escalation study of carbon ion radiotherapy for locally advanced head-and-neck cancer.** *Int J Radiat Oncol Biol Phys* 2004, **60**:358–364.
11. Endo M, Koyama-Ito H, Minohara S, Miyahara N, Tomura H, Kanai T, Wawachi K, Tsujii H, Morita K: **HIPLAN - A heavy ion treatment planning system at HIMAC.** *J Jpn Soc Ther Radiol Oncol* 1996, **8**:231–238.
12. Kanai T, Endo M, Minohara S, Miyahara N, Koyama-ito H, Tomura H, Matsufuji N, Futami Y, Fukumura A, Hiraoka T, Furusawa Y, Ando K, Suzuki M, Soga F, Kawachi K: **Biophysical characteristics of HIMAC clinical irradiation system for heavy-ion radiation therapy.** *Int J Radiat Oncol Biol Phys* 1999, **44**:201–210.
13. Amirul Islam M, Yanagi T, Mizoe JE, Mizuno H, Tsujii H: **Comparative study of dose distribution between carbon ion radiotherapy and photon radiotherapy for head and neck tumor.** *Radiat Med* 2008, **26**:415–421.
14. Morrish RB, Chan E, Silverman S, Meyer J, Fu KK, Greenspan D: **Osteoradionecrosis in patients irradiated for head and neck carcinoma.** *Cancer* 1981, **48**:1980–1983.
15. Katsura K, Sasai K, Sato K, Saito M, Hoshina H, Hayashi T: **Relationship between oral health status and development of osteoradionecrosis of the mandible: a retrospective longitudinal study.** *Oral Surg Oral Med Oral Pathol Oral Radiol Endod* 2008, **105**:731–738.

doi:10.1186/1748-717X-9-92
Cite this article as: Sasahara *et al.*: Effects of the dose-volume relationship on and risk factors for maxillary osteoradionecrosis after carbon ion radiotherapy. *Radiation Oncology* 2014 **9**:92.

Carbon ion radiotherapy for locally advanced squamous cell carcinoma of the external auditory canal and middle ear

Masashi Koto, MD, PhD[a], Azusa Hasegawa, DDS, PhD[a], Ryo Takagi, DDS, PhD[a], Go Sasahara, MD, PhD[a], Hiroaki Ikawa, DDS, PhD[a], Jun-etsu Mizoe, MD, PhD[b], Keiichi Jingu, MD, PhD[c], Hirohiko Tsujii, MD, PhD[a], Tadashi Kamada, MD, PhD[a], Yoshitaka Okamoto, MD, PhD[d], and Organizing Committee for the Working Group for Head-and-Neck Cancer

[a]Research Centre for Charged Particle Therapy Hospital, National Institute of Radiological Sciences, Chiba, Japan

[b]Nagoya Proton Therapy Center, Nagoya, Japan

[c]Department of Radiation Oncology, Tohoku University School of Medicine, Sendai, Japan

[d]Department of Otolaryngology, Chiba University School of Medicine, Chiba, Japan

Corresponding author: Masashi Koto, M.D., Ph.D., Research Centre for Charged Particle Therapy Hospital, National Institute of Radiological Sciences, Anagawa 4-9-1, Inage-ku 263-8555 Chiba, Japan. Tel: +81-43-206-3360; Fax: +81-43-256-6506; Email: koto@nirs.go.jp

Study support: This study was supported by the Research Project with

Heavy Ions at the National Institute of Radiological Sciences (NIRS)–Heavy Ion Medical Accelerator in Chiba (HIMAC).

Running title: C-ion RT for SCC of the ear

Key words: carbon ion radiotherapy, squamous cell carcinoma, external auditory canal, middle ear, temporal bone.

Abstract

Background: The prognosis of advanced squamous cell carcinoma (SCC) of the external auditory canal (EAC) and middle ear (ME) remains poor. Carbon ion radiotherapy (C-ion RT) has shown promise for locally advanced head and neck cancer. Therefore, we evaluated the safety and efficacy of C-ion RT for locally advanced SCC of the EAC and ME.

Methods: The cases of 13 patients with advanced (T3 and T4) SCC of the EAC and ME who received C-ion RT as the primary treatment were reviewed.

Results: The median follow-up for all patients and the seven surviving patients was 12 and 32 months, respectively. The 1-year and 3-year local control and overall survival rates were 72% and 54% and 70% and 40%, respectively. Severe temporal bone necrosis was observed in two patients.

Conclusion: C-ion RT is effective and generally safe for locally advanced SCC of the EAC and ME.

Introduction

Carcinomas of the external auditory canal (EAC) and middle ear (ME) are rare. The incidence is estimated to be 1 to 6 patients per million populations per year[1-3]. Squamous cell carcinoma (SCC) is the most common histological subtype. There is no universal consensus on the optimal treatment for SCC of the EAC and ME because of its scarcity. However, in general, the following standard treatments are used for SCC classified according to the Pittsburgh staging system[4]: surgery or radiotherapy for T-classification (T)1 tumors and surgery with or without radiotherapy for T2, T3, and T4 tumors.

Although excellent clinical results for patients with early-stage SCC of the EAC and ME have been reported[5-8], the prognosis of patients with advanced-stage disease, particularly T4, remains poor. Xie et al.[9] found that, in a series of 39 patients with temporal bone SCC treated with surgery with radiotherapy, the 2-year overall survival (OS) rate was 22.3% for patients with T4 tumors or positive lymph nodes. Moreover, in a multi-institutional retrospective review, Ogawa et al.[8] reported a 1-year disease-free survival (DFS) rate of 0% in 16 patients with T3 or T4 SCC of the EAC and ME treated with radiotherapy alone.

Carbon ion radiotherapy (C-ion RT) was initiated at the National Institute of Radiological Sciences (NIRS) in 1994. C-ions exhibit high linear energy transfer and display good dose-localizing properties compared with other ion species and photons[10, 11]. Therefore, C-ion RT

is expected to be effective for radioresistant tumors. For cancers in the head and neck region, C-ion RT is mainly performed for non-SCCs such as salivary gland carcinoma and mucosal malignant melanoma. C-ion RT has shown promising results for locally advanced head and neck cancer in a phase II clinical trial[12, 13]. SCC of the head and neck region is generally radiosensitive; however, radiotherapy is often unable to control locally advanced SCC of the EAC and ME. Therefore, C-ion RT may be a viable treatment option for locally advanced SCC of the EAC and ME.

Accordingly, the objective of this study was to evaluate the effectiveness and safety of C-ion RT for patients with locally advanced SCC of the EAC and ME.

Materials and Methods

The treatment protocol for head and neck cancer was reviewed and approved by the NIRS Ethical Committee on Human Clinical Research, and all patients provided written informed consent. A retrospective case review was undertaken of all patients with SCC of the EAC and ME who were treated with C-ion RT at the NIRS between June 1997 and May 2013. A total of 13 patients were enrolled in the study. All patients received C-ion RT as a primary treatment.

Patient and treatment characteristics are summarized in Table 1. All primary tumors were classified according to the Pittsburgh staging

system. Before treatment, 3 patients had T3 disease, and 10 patients had T4 disease. Patients with metastatic lymph nodes that were localized around the primary tumor were included. Lymph node status and distant metastasis were classified using the TNM staging system for cancers of the head and neck region. Two patients were classified as N1 and 1 patient as N2b. All patients were classified as M0.

Carbon ion radiotherapy

Doses of carbon ions were expressed in photon-equivalent doses (Gray equivalent [GyE]), defined as the physical doses multiplied by the relative biological effectiveness (RBE) of the carbon ions[10]. The biological flatness of the spread-out Bragg peak (SOBP) was normalized by the survival fraction of the human salivary gland tumor cells at the distal region of the SOBP, where the RBE of carbon ions was assumed to be 3.0. C-ion RT was administered on a fractionation schedule comprised of 64.0 GyE/16 fractions for 4 weeks. When a wide range of skin or mucosa was included in the target volume, a dose of 57.6 GyE/16 fractions for 4 weeks was used.

The patients were positioned in customized cradles (Moldcare; Alcare, Tokyo, Japan) and immobilized using a low-temperature thermoplastic shell (Shellfitter; Kuraray, Osaka, Japan). A set of computed tomography (CT) images of 2.5-mm thickness was obtained for treatment planning with the immobilization devices. Magnetic resonance imaging (MRI), after fusing with the planning CT image, was

routinely used for identification of the tumor. Determination of the gross tumor volume (GTV) was based on contrast-enhanced MRI. The clinical target volume (CTV) had a minimum margin of 5 mm added around the GTV. In cases with possible tumor invasion into adjacent sites, CTV1 included whole anatomical sites, and CTV2 was limited to the GTV. The planning target volume (PTV)1 and PTV2 had margins of 3–5 mm added around the CTV1 and CTV2, respectively. The PTV1 was irradiated initially with 36 GyE/9 or 10 fractions and thereafter, PTV2 was irradiated to a total dose of 64.0 or 57.6 GyE/16 fractions. The target reference point dose was defined as the isocentre, and the PTV was encompassed by the minimum 90% dose line of the reference point dose. The CTV and PTV margins of areas close to the brain and skin were reduced as necessary.

Multiportal irradiation was planned fundamentally to avoid severe normal tissue reactions. Three-dimensional treatment planning was performed using original HIPLAN software.

During C-ion RT, patients received no concomitant therapy, and after completion, patients received no adjuvant therapy such as surgery or chemotherapy. No patients received prophylactic neck irradiation. Treatment methods for local recurrence and distant metastasis had no limitations.

Evaluation and follow-up examinations

All patients underwent a CT and MRI examination before treatment to

determine clinical stage. Acute reactions in normal tissues were classified according to the Radiation Therapy and Oncology Group scoring system. Late reactions were classified according to the National Cancer Institute Common Terminology Criteria for Adverse Effect version 4.0. Local control (LC) was defined as no evidence of tumor regrowth in the PTV1. Regional control was defined as no evidence of recurrence in both the temporal bone outside of the PTV1 and regional lymph nodes. Oncological status was followed using CT or MRI every 2–3 months for the first 2 years after C-ion RT and every 3–6 months thereafter.

Statistical analyses

LC, OS, and DFS rates were determined using the Kaplan-Meier method and compared among the different subgroups using the log-rank test. All analyses were calculated from the first day of C-ion RT. A P value below 0.05 was considered significant. Statistical analyses were performed using SPSS software version 11 (SPSS Inc., Chicago, IL, USA).

Results

Local control and survival

The median observation period was 12 months (range, 2–80 months) for all patients and 32 months (range, 2–80 months) for the 7 surviving patients. No patients were lost to follow-up.

The 1-year and 3-year LC rates were 75.2% (95% confidence interval [CI] = 50.6–99.8%) and 56.4% (95% CI = 19.5–93.3%), respectively (Fig. 1). Four patients developed local recurrence. Of the three patients who developed regional recurrence, two patients had local recurrence. Of the two patients who developed distant metastasis, one patient had local recurrence. A representative case is shown in Fig. 2.

The 1-year and 3-year OS rates were 72.7% (95% CI = 46.4–99.1%) and 41.6% (95% CI = 10.9–72.2%), respectively. The 1-year and 3-year DFS rates were 49.9% (95% CI = 20.9–78.9%) and 37.4% (95% CI = 7.0–67.7%), respectively (Fig. 3). Of the six patients who died, five patients died of their original disease, and one patient died of intercurrent disease without recurrence.

Univariate analysis of risk factors for local control and survival

Table 2 shows the results of the univariate analysis of risk factors for LC and OS. Young age was a significant risk factor for LC. Male gender and young age were risk factors for OS. Tumor and treatment characteristics were not significant risk factors for LC or OS.

Toxicity

Acute skin reactions to C-ion RT occurred. Grade 1, grade 2, and grade 3 skin reactions were observed in five patients, six patients, and two patients, respectively. Severe vertigo and tinnitus did not occur during C-ion RT.

Regarding late reactions, two patients who were treated with a

total dose of 57.6 GyE developed grade 3 temporal bone necrosis with skin ulcer. Of these two patients, one died from distant metastases without local recurrence, and the other died from intercurrent cause. Four patients were judged to have maximum grade 2 brain injuries. These patients developed localized brain necrosis. However, mild headache was the only clinical symptom, which eventually disappeared. All patients had tumor-induced hearing impairment before C-ion RT. The hearing impairment did not improve or progressed after C-ion RT. Tinnitus and vertigo above grade 2 were not observed. Five patients showed tumor-related facial nerve palsy before C-ion RT. However, none of the patients developed treatment-related facial nerve palsy.

Discussion

The gold standard for treating advanced SCC of the EAC and ME is surgery with radiotherapy. However, the role of radiotherapy is limited for macroscopic residual tumors. In a multi-institutional study, Yin et al.[14] demonstrated that adjuvant radiotherapy provided a 5-year survival rate of 20.8% for EAC and ME SCC patients with positive surgical margins, which was significantly lower than the 5-year survival rate of 76.5% for patients with negative surgical margins. Moreover, Ogawa et al.[9] reported that the DFS rate of T3 or T4 tumors treated with radiotherapy alone was 0% at 1 year. In our study, C-ion RT was found to be an effective treatment for advanced SCC of the EAC and ME, with

1-year LC, OS, and DFS rates of 75.2%, 72.7%, and 49.9%, respectively. Our findings suggest that C-ion RT has a greater biological effectiveness than radiotherapy and may be a viable treatment option for locally advanced SCC of the EAC and ME, especially for unresectable tumors.

Few studies have reported radiation-induced late complications for advanced SCC of the EAC and ME. Ogawa et al.[9] reported that, of 87 patients with SCC of the EAC and ME, one patient each developed grade 4 osteoradionecrosis and grade 4 skin ulcer after radiotherapy. Leong et al.[15] observed late complications including trigeminal neuralgia, mandible osteoradionecrosis, postauricular sinus, and epilepsy in 35 patients treated with surgery and postoperative radiotherapy. In our study, two (15%) patients developed grade 3 temporal bone necrosis with skin ulcer and were treated at the beginning of C-ion RT. The temporal bone necrosis may have been exacerbated by the infection from the skin ulcer. The PTVs in these retrospective cases were larger than the current typical PTV, and the skin was not sufficiently spared. Four of the eight patients with skull base invasion developed symptomatic brain necrosis. However, the necrotic brain areas were localized because of the superior dose distribution of C-ions, and consequently, the clinical symptoms were mild. Moreover, we recently reported that brain volume receiving more than 50 GyE (V50) was a significant predictive factor for the development of brain necrosis after C-ion RT using a 16-fraction regimen[16]. Monitoring V50 may predict or